Supporting Information

Single-shot Optical Anisotropy Imaging with Quantitative Polarized Interference Microscopy

Baoliang Ge,[1,2,3,†] Renjie Zhou,[4, †,] Yu Takiguchi,[5] Zahid Yaqoob,[3,*] Peter T. C. So.[1,2,3]*

[1]Department of Mechanical Engineering, Massachusetts Institute of Technology, Cambridge, Massachusetts, 02139, USA
[2]Department of Biological Engineering, Massachusetts Institute of Technology, Cambridge, Massachusetts, 02139, USA
[3]Laser Biomedical Research Center, Massachusetts Institute of Technology, Cambridge, Massachusetts, 02139, USA
[4]Department of Biomedical Engineering, The Chinese University of Hong Kong, Shatin, New Territories, Hong Kong SAR, China
[5]Central Research Laboratory, Hamamatsu Photonics K.K, Hamamatsu, Shizuoka, 434-8601, Japan

[†]These authors contributed equally to this work
[*]Corresponding Authors: e-mail: rjzhou@cuhk.edu.hk and zyaqoob@mit.edu

This document provides supplementary information for the article 'Single-shot quantitative optical anisotropy imaging with polarized interference microscopy'. The first part illustrates the retrieval of the complex field and the 0^{th} order amplitude from the recorded interferogram. The second part shows a theoretical analysis of QPIM measurement sensitivity. The third part provides a temporal noise analysis of our QPIM system, whereas the last part presents a spatial noise analysis of our QPIM system.

1. The Retrieval of Complex Field

The Fourier transform of Equation 9 is:

$$\begin{aligned} I(u,v) &= \Im_{2D}\left[I(x,y)\right] \\ &= \left[\tau(u,v)\otimes I_{in}(u,v)\right]\otimes\left\{2\delta(u,v)\right. \\ &\quad -\frac{1}{2}\Im_{2D}\left[\cos 2\varphi(x,y)\sin\Delta(x,y)\right]\otimes \\ &\quad \left[\delta(u-u_0,v)+\delta(u+u_0,v)\right] \\ &\quad \left.+\frac{i}{2}\Im_{2D}\left[\cos\Delta(x,y)\right]\otimes\left[\delta(u-u_0,v))-\delta(u+u_0,v)\right]\right\}, \end{aligned} \tag{S1}$$

where (u,v) represents the 2D Fourier space of (x,y) ; $\Im_{2D}$ represents the 2D Fourier transform; $\otimes$ represents the 2D convolution; $\delta(u,v)$ is a 2D delta function. As seen from Eq. (S1), there are 0[th] and 1[st] order terms in the frequency domain, and each order contains the birefringence parameters. A mask $M(u,v)$ is used to numerically extract the 0[th] and 1[st] order signals under the restriction of the numerical aperture of the system[1]. For selecting the 1st order (centered at $u=u_0$, where $u_0 = k/2\pi$), we let $M(u,v)=1$ when $\sqrt{(u-u_0)^2+v^2} < NA/\lambda$, and $M(u,v)=0$ for all other regions. After extracting the 1[st] order signal, we shift it back to the origin, which gives the complex electric field:

$$\begin{aligned} U(u,v) &= \left[\tau(u,v)\otimes I_{in}(u,v)\right] \\ &\quad \otimes\Im_{2D}\left[\cos 2\varphi(x,y)\sin\Delta(x,y)-i\cos\Delta(x,y)\right]. \end{aligned} \tag{S2}$$

With a 2D inverse Fourier transform, $U(x,y)$ is obtained as written in Equation 10. The 0[th] order can be extracted as:

$$A(u,v) = 2\tau(u,v)\otimes I_{in}(u,v). \tag{S3}$$

Therefore, the distribution of the 0[th] order signal in the spatial domain is obtained as described by Equation 11.

2. Sensitivity Analysis for QPIM

Like other quantitative phase microscope designs, the measurement sensitivity of QPIM can be affected by many environmental factors, such as mechanical vibrations or air density fluctuations. However, when these environmental influences are minimized, the effect of shot noise becomes dominant. According to Poisson statistics, the minimum temporal standard deviation of the intensity can be expressed as:

$$\delta I = \frac{1}{\sqrt{N}}, \tag{S4}$$

where is the well depth of the camera. For interferograms of near-common-path setups, the intensity distributions can be expressed by (note that for simplicity we consider a one-dimensional signal, but it can be easily extended to 2D signals):

$$I(x) = I_0 \left\{ 1 + \gamma(x) \cos\left[\frac{2\pi}{\Lambda} x + \bar{\phi}(x) \right] \right\}. \tag{S5}$$

where $I(x)$ denotes the interferogram distribution, I_0 is the average value of the intensity(assume the illumination I_{in} is uniform and the sample's absorption τ is negligible), $\gamma(x)$ and $\bar{\phi}(x)$represent the amplitude and phase of the detected complex field, and is the spatial period of the interferogram. $\bar{\phi}(x)$ is actually the differential phase of two sample beams. Based on our algorithm, we can retrieve the 0^{th} order intensity (i.e., DC term), the real part, and the imaginary part of complex field which can be shown as:

$$
\begin{aligned}
A(x) &= I_0, \\
B(x) &= \frac{1}{2}\gamma(x) I_0 \cos\phi_s(x), \\
C(x) &= \frac{1}{2}\gamma(x) I_0 \sin\phi_s(x).
\end{aligned}
\tag{S6}
$$

In **Figure S1**a, we described a simple situation that four camera pixels sample each period of the fringes. We also assume that $I_0 = \frac{1}{2}, \gamma(x) = 1, \phi_s(x) = 0$. The intensities of each pixel are $I_1 = 1, I_3 = 0, I_2 = I_4 = 1/2$. Therefore, based on previous analysis[2], A, B, and C can be retrieved as:

$$
\begin{aligned}
A &= \frac{1}{4}(I_1 + I_2 + I_3 + I_4) = \frac{1}{2}, \\
B &= \frac{1}{2}\frac{I_1 - I_3}{2} = \frac{1}{4}, \\
C &= \frac{1}{2}\frac{I_2 - I_4}{2} = 0.
\end{aligned}
\tag{S7}
$$

Since the intensity of each pixel is proportional to the number of photons received, following the Poisson statistics the measurement uncertainties of A, B, and C are

$$
\delta^2 A = \frac{1}{4}(\delta^2 I_1 + \delta^2 I_2 + \delta^2 I_3 + \delta^2 I_4) \geq \delta^2 I = \frac{1}{N},
\tag{S8}
$$

$$
\begin{aligned}
\delta^2 B &= \frac{1}{4}\delta^2(I_1 - I_3) = \frac{1}{4}\frac{\delta^2(n_1 - n_3)}{(n_1 - n_3)^2} \\
&= \frac{1}{4}\frac{1}{n_1 - n_3} \geq \frac{1}{4N},
\end{aligned}
\tag{S9}
$$

$$
\begin{aligned}
\delta^2 C &= \frac{1}{4}\delta^2(I_2 - I_4) = \frac{1}{4}\frac{\delta^2(n_2 - n_4)}{(n_2 - n_4)^2} \\
&= \frac{1}{4}\frac{1}{n_2 - n_4} \geq \frac{1}{4N},
\end{aligned}
\tag{S10}
$$

We can see that the optimal variances of both B and C equal 1/4N. The DC term of the interferogram, A is the spatial average of the interferogram. We can also assume its uncertainty is the same as the interferogram as shown in Equation S8. Therefore, we can conclude that the optimal standard deviations are:

$$\delta A = \delta I = \frac{1}{\sqrt{N}}, \delta B = \delta C = \frac{\delta I}{2} = \frac{1}{2\sqrt{N}}. \tag{S11}$$

According to the result shown in Equation S9 and the principles of error propagation[3], the uncertainties of recovered retardance and orientation angle are shown below:

$$\delta^2 \Delta = \frac{1}{2A^2}\left(\frac{A+8C^2}{A-4C^2}\right)\delta^2 I, \tag{S12}$$

$$\delta^2 \varphi = \left(\frac{(A^2+8B^2)(A^2-4C^2)^2+16B^2C^2(A^2+8C^2)}{2A^2(A^2-4B^2-4C^2)(A^2-4C^2)^2}\right)\delta^2 I. \tag{S13}$$

Based on Equations 11-13, if we assume the transmittance τ of the sample and the illumination intensity distribution I_{in} is uniform, we can rewrite the DC term A, real part B, and imaginary part C from the given values of retardance Δ and orientation angle φ. Therefore, the standard deviations of varying retardance and orientation angle can be simulated, which are shown in Figures S1b-d, where we assume the well depth of the camera is 10651 electrons. For the measurement of retardance, the uncertainty is only related to its own actual values. As shown in Figure S1b, the retardance measurement is the most accurate when the actual retardance is π/2 with a standard deviation of 0.014 rad. However, the uncertainty becomes singular when the actual retardance is 0 or π, which means the measurement is not reliable when the anisotropic signal is very weak. For the measurement of orientation angle the situation is more complicated. Its uncertainty relies on both retardance

and orientation angle values. The standard deviation of orientation angle becomes singular when the retardance is 0 or π, which is shown in Figure S1c. It is reasonable because when the retardance is zero, the measured orientation angle value has no physical meaning (i.e., the sample is essentially isotropic). The standard deviation of orientation is also related to the orientation angle itself, which is shown in Figure S1d where the retardance is fixed at π/2. The uncertainty is singular when the orientation angle is 0 or 90 degrees, which means the measurement of orientation is not reliable when it is parallel to x or y axis defined by the Wollaston orientation. The optimal sensitivity orientation angle is 0.79 degree (0.014 rad) when the retardance is π/2, and the orientation angle is 45 or 135 degrees. However, these simulated results assume that the depth well is depleted in every pixel of the camera, which is impossible in actual measurements. Therefore, the measured temporal noise is always larger than the calculated one. But we can still learn the trend of the shot noise variation on the dependency of the measured retardance and orientation angles with the simulation results.

3. Temporal Noise Analysis

To experimentally analyze the temporal uncertainty of the QPIM system, we measured 900 consecutive interferograms on the LCD sample at 150 fps imaging speed while no voltage is applied (this ensures that the retardance is uniform over the whole field of view). After acquiring the interferograms, we retrieved the 0^{th} order intensity (A), and the real part (B) and the imaginary part (C) of the 1^{st} order complex field, and then recover the retardance and the orientation angle distributions based on our algorithms (refer to Method Section A). We pick the sample pixel of each image, record their variations over time. In this way, we can obtain the time lapse and analyze their temporal uncertainties. As shown in **Figure S2**a, the standard deviation of the 0th order intensity (A), and the real part (B) and the imaginary part

(C) of the retrieved complex field is 0.011, 0.005 and 0.005, respectively. The well depth for the camera is 10651 electrons, which means that the intensity standard deviation due to the photon shot-noise is 0.0097. The experimentally measured values are slightly larger than expected values of 0.0097 (for A), 0.0049 (for B), and 0.0049 (for C). The reason may be that the electron well is not fully filled. In Figure S2b, the temporal uncertainties of the recovered retardance and orientation angle are also experimentally measured, which are 0.04 rad and 2.05 degrees respectively. Also, the histograms of retrieved retardance and orientation angle time series are shown in Figures S2c and d. The measured value of retardance and orientation angle are 0.3π rad and 30.6 degrees. From the theoretical frame mentioned in Equations S12-S13, the corresponding uncertainties for retardance and orientation angle are 0.02 rad and 1.3 degrees. The discrepancies may also due to the insufficiency filling the electron well factors and other systematic errors rooted in the current QPIM system. Nevertheless, we should be mindful that the birefringence uncertainties are dominated by the photon shot noise, which can be only improved by using higher well depth cameras.

4. Spatial Noise Analysis

To determine the spatial noise of birefringence measurements using our system, we calculated the standard deviation of the a fixed 200 × 200-pixel region in the recovered retardance, orientation angle, and unwrapped retardance maps. The distributions are measured from the nematic liquid crystal sample, and a uniform region as indicated by white boxes in Fig. S3 is used for calculating the spatial uncertainty values. **Figure S3**a, c, and e show the recovered retardance, orientation angle, and the unwrapped retardance distributions, respectively. Histograms corresponding to the white box regions are generated as shown in Figure S3b, d, and f. From the histograms, we determined that the standard deviation of retardance,

orientation angle, and unwrapped retardance are 0.0061 rad, 0.40 degrees, and 0.0031 rad. Those values, if translated into optical path differences, are within 0.3-0.6 nm.

References

[1] B. Bhaduri, C. Edwards, H. Pham, R. Zhou, T. H. Nguyen, L. L. Goddard, G. Popescu, Diffraction phase microscopy: principles and applications in materials and life sciences. *Advances in Optics and Photonics* **2014**, 6 (1), 57-119.

[2] P. Hosseini, R. Zhou, Y. H. Kim, C. Peres, A. Diaspro, C. Kuang, P. T. C. So, Pushing phase and amplitude sensitivity limits in interferometric microscopy. *Optics Letters*, **2016** 41(7), 1656-1659.

[3] J. Stoer, R. Bulirsch, *Introduction to numerical analysis*. *Chapter1: Error analysis*. Vol. 12, 1-36 (Springer Science & Business Media, 2013).

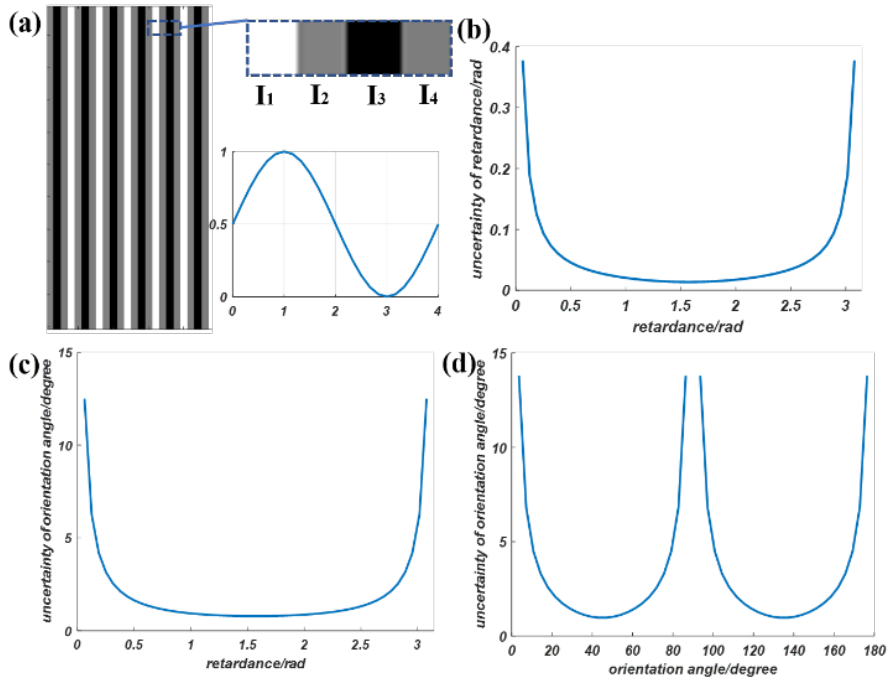

Figure S1. Theoretical analysis of QPIM sensitivity. (a) The sketch of the interferogram intensity distribution relative to the well depth of the camera; (b) the relation of the recovered retardance's standard deviation and the actual value of it; (c) the relation of the recovered orientation angle's standard deviation and the actual value of retardance; (d) the relation of the recovered orientation angle's standard deviation and its own actual values.

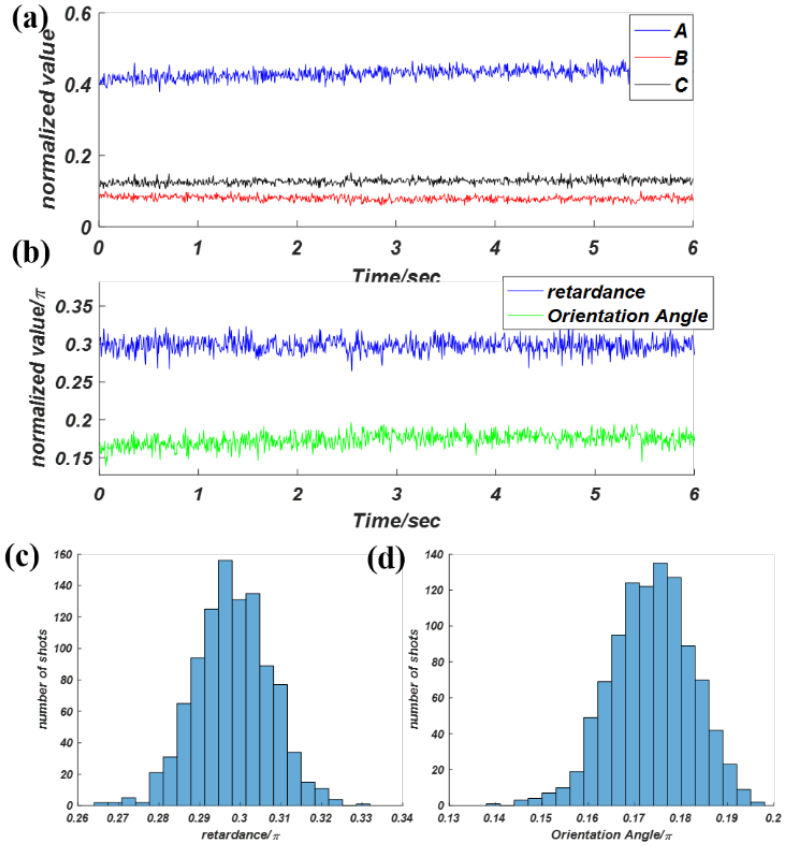

Figure S2. Time lapse of birefringence parameters and temporal noise analysis. (a) The time lapse plots of the recovered 0th order intensity(A), and the real part (B) and imaginary part(C) of +1st complex field. (b) The time lapse plots of the retardance and orientation angle. The recording period is 6 seconds at 150 fps (c) the histograms of the retardance and (d) orientation angle time series. The unit of retardance and orientation angle is radiance and divided by π.

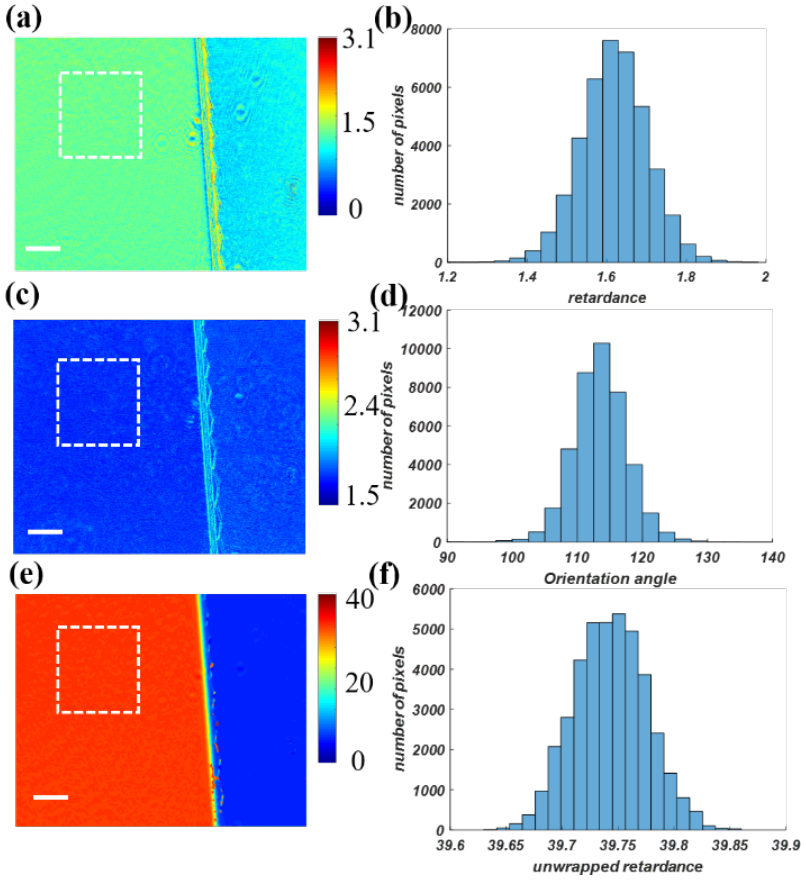

Figure S3. Spatial uncertainty analysis of the measured birefringence parameter on a uniform LC region. (a) The recovered retardance distribution; (b) the histogram of the region marked with dashed white line in (a); (c) the recovered orientation angle distribution; (d) the histogram of the white dashed line marked region in (c); (e) the unwrapped retardance distribution; (f) the histogram of the white dashed line marked region in (e).